JOURNAL OF AGRICULTURAL AND FOOD CHEMISTRY

pubs.acs.org/JAFC Article

Microbial Transformations of Two Beyerane-Type Diterpenes by *Cunninghamella echinulata*

Yu-Qi Gao, Ruoxin Li, Wei-Wei Wang, Shoei-Sheng Lee, and Jin-Ming Gao*

Cite This: *J. Agric. Food Chem.* 2020, 68, 4624–4631 Read Online

ACCESS | Metrics & More | Article Recommendations | Supporting Information

ABSTRACT: Microbial transformations of two tetracyclic beyerane-type diterpenes, *ent*-16β-oxobeyeran-19-oic acid (**1**) and its chemical reduction product, *ent*-16β-hydroxybeyeran-19-oic acid (**2**), by the filamentous fungus *Cunninghamella echinulata* ATCC 8688a yielded eight metabolites (**3**−**10**). Incubation of the substrate **2** with *C. echinulata* afforded three new hydroxylated ones (**3**−**5**) along with two known ones (**6**−**7**), while incubation of **1** gave three known ones (**8**−**10**). The new compounds were characterized by 1D and 2D NMR as well as HRESIMS analysis, and the stereostructures of **3** and **4** were confirmed by X-ray crystallography. The bioreactions were involved not only in stereoselective incorporation of hydroxyl groups at inert positions C-7, -9, -12, and -14 of the two beyerane diterpenes but also in glucosidation at C-19 of **2**. This is the first report on the biotransformation of the diterpenes by using *C. echinulata*. All compounds were assayed for their α-glucosidase inhibitory, neurotrophic, anti-inflammatory, and phytotoxic activity, and only in neurotrophic assay compounds, **2** and **9** were found to display nerve growth factor-mediated neurite-outgrowth promoting effects in PC12 cells; the others were inactive.

KEYWORDS: *beyerane diterpenes, biotransformation, Cunninghamella echinulata, biocatalysis, hydroxylation*

INTRODUCTION

Stevioside, isolated from the leaves of *Stevia rebaudiana* (family Asteraceae), is commonly utilized as a non-caloric natural sugar substitute in many kinds of foods and as food supplements in many countries.[1] Stevioside is a complex diterpenoid glycoside molecule and was hydrolyzed under alkaline or acidic conditions to generate the stevioside aglycone, *ent*-kaurane diterpene steviol or *ent*-beyerane diterpene isosteviol (**1**), respectively. Steviol and isosteviol have been demonstrated to have many biological properties, such as anti-inflammatory, anti-hypertensive, anti-diabetes, anticancer, and neuroprotective properties.[1−3]

Microbial transformations have been proved a useful means for incorporating hydroxyl groups at non-activated positions in the diterpenoid or steroid scaffold for structural modifications.[4−7] Diterpenoids are a diverse group of bioactive components found in several plant-derived extracts. Structure modifications of the diterpenoids to increase their pharmaceutical relevance can be efficiently performed by the use of biotransformation processes utilizing microbes or isolated enzymes.[5] In addition, the microbial biotransformation has many advantages: to surmount the problems present in organic synthesis reactions; to enhance/reduce the biological activity/toxicity profiles of the drugs; and to mimic mammalian drug metabolism.[8,9] Taking into account that small changes in a molecular structure may significantly affect its bioactivities and properties, although these two diterpenoids shows many attractive bioactivities, their poor water solubility limits further application. In spite of several semisynthesis and structure modifications of isosteviol that have been described, investigations on several diterpenoids derived from biotransformation of isosteviol (**1**) and new biological activities have so far been limited.[10−14]

In order to study the metabolism of the two tetracyclic beyerane-type diterpenes, isosteviol (*ent*-16β-oxobeyeran-19-oic acid, **1**) and its chemical reduction product (*ent*-16β-hydroxybeyeran-19-oic acid, **2**) and to predict their likely mammalian metabolites, in the current work, biotransformation of these two diterpenoids by the fungal strain *Cunninghamella echinulata* ATCC 8688a was carried out, leading to the isolation and identification of eight metabolites (**3**−**10**) (Scheme 1) from the fermentation broth. Herein, we deal with the microbial conversion of **1** and **2** and isolation, structure elucidation, and biological evaluation of several metabolites.

MATERIALS AND METHODS

General Experimental Procedures. The specific rotation was measured on a JASCO DIP-370 polarimeter. IR spectra were recorded on a JASCO FT/IR-410 FT-IF spectrometer. 1D- and 2D-NMR spectra were obtained on a Bruker Avance 400 or Avance III 500 or 600 Cryo-probe spectrometer (Bruker Instruments, UK), operating at 400, 500, and 600 MHz (^{1}H) and 100, 125, and 150 MHz (^{13}C) in methanol-d_4 using the signals of the residual solvent protons (δ_H 3.30) and carbons (δ_C 49.0) as internal standards. Electrospray ionization mass spectra (ESIMS) were recorded on a Bruker Daltonics Esquire 2000 ESI-Ion Trap Mass Spectrometer or

Received: January 28, 2020
Revised: March 23, 2020
Accepted: March 25, 2020
Published: March 27, 2020

https://dx.doi.org/10.1021/acs.jafc.0c00592
J. Agric. Food Chem. 2020, 68, 4624−4631

Scheme 1. Chemo- and Biotransformations of Stevioside and Its Derivatives Isosteviol (1) and *ent*-16β-Hydroxybeyeran-19-oic Acid (2)

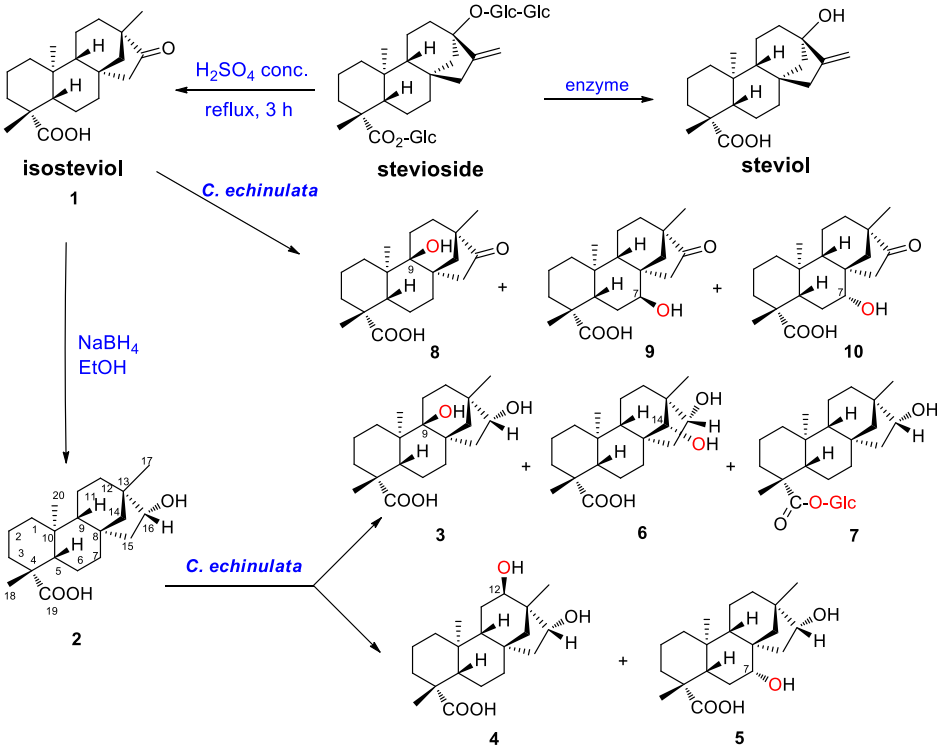

Bruker Daltonics microTOF II Mass Spectrometer and Thermo Scientific Q Exactive HF Orbitrap-FTMS. Column chromatography (CC) was carried out on 200−300 mesh silica gel (Qingdao Marine Chemical Ltd., Qingdao, P. R. China), RP-18 (40−63 μM; Merck, Darmstadt, Germany), and Sephadex LH-20 (20−100 μm; Amersham Biosciences, Uppsala, Sweden). Thin layer chromatography (TLC) analysis was performed on precoated Si gel 60 GF_{254} (Qingdao Marine Chemical Ltd.). Developed chromatograms were visualized by spraying developed plates with 5% H_2SO_4 in EtOH and then by heating until maximum development of the spot colors. All reagents and solvents used were of analytical grade.

Semisynthesis of Compounds 1 and 2. The substrates isosteviol (**1**) and *ent*-16β-hydroxybeyeran-19-oic acid (**2**) were derived from stevioside as described previously[10,12] and were confirmed by NMR and ESIMS data.

Microorganisms and Culture Medium. The microbes employed in this work included *Geotrichum candidum* ATCC 34614, *Rhizopus stolonifer* ATCC 6227a, *Rhizopus chinensis* CCTCC M201021, *Apergillus ochraceus*, *Aspergillus niger* CICC2377, *Cunninghamella blakesleeana* CGMCC 3.970, *Cunninghamella elegans* ATCC 36112, *C. echinulata* ATCC 8688a, *Penicillium citrinum* ATCC 8506, *Mucor mucedo* CBS228.29, and *Mucor wutungchiao* CBS 111557. They were screened for their abilities to convert substrates **1** and **2** in preliminary work. These microorganisms were maintained on potato-dextrose agar media slants at 4 °C. Before the conversion experiments, all organisms were freshly subcultured. Preliminary screening bioconversion of **1** or **2** by *C. echinulata* ATCC 8688a was carried out by a two-stage fermentation procedure in potato-dextrose medium. The medium was autoclaved at 121 °C for 30 min before use.

Culture Conditions and Biotransformation Procedures. The microorganisms were inoculated in 250 mL Erlenmeyer flasks containing 50 mL of potato-dextrose medium. The flasks were incubated at 28 °C on a rotary shaker at 180 rpm for 48 h. The solution of compound **1** in acetone (10 mg/mL) was added to each flask. Final concentration of **1** in this media was 0.1 mg/mL, and incubation was continued for 5 d. Both parallel controls, the substrate control (substrate in organism-free culture medium) and culture control (organisms in substrate-free culture medium), were incubated under the same conditions to show the stability of the substrate in the process of incubation. The results of the transformation were monitored by TLC. Similarly, a preparative-scale biotransformation by *C. echinulata* ATCC 8688a was conducted in 500 mL Erlenmeyer flasks containing 200 mL of potato-dextrose media, and the microorganisms were precultured for 2 d.

Bioconversion of **2** by *C. echinulata* ATCC 8688a was carried out following the aforementioned procedures of **1**. Compound **2** (2.8 g) was dissolved in acetone (280 mL), and final concentrations of 0.1 mg/mL were distributed among the medium.

Extraction and Isolation. The fermentation cultures of **2** were pooled and filtered, and the obtained mycelia were ultrasonically washed three times with EtOAc. The filtrates were extracted thrice with an equal volume of EtOAc. The combined organic layer was dried over anhydrous Na_2SO_4, filtered, and evaporated *in vacua* to give a brown oil. The residue (3.98 g) was submitted to silica gel CC and eluted with a gradient of $CHCl_3$−CH_3OH (100:0, 98:2, 95:5, 92:8, 90:10, 80:20) to provide fractions A−F. Fraction C was subjected to CC over silica gel and eluted with $CHCl_3$−CH_3OH (95:5) to provide four fractions (Fr.C1−4). Fr.C1 (361 mg) was fractionated by a Sephadex LH-20 column (CH_3OH), silica gel CC with $CHCl_3$−CH_3OH (98:2), followed by recrystallization from CH_3OH, to afford compound **3** (41 mg). Fr.C3 (202 mg) was fractionated by a Sephadex LH-20 column with $CHCl_3$−CH_3OH (1:1), silica gel CC with $CHCl_3$−CH_3OH (96:4), followed by a RP-18 column using CH_3OH−H_2O (30:70, 40:60, 50:50, 60:40, 30:70, 80:20). Compound **4** (16 mg) from subfraction eluted with CH_3OH−H_2O (50:50) was purified by Sephadex LH-20 CC (CH_3OH), and **6** (16.6 mg) from subfraction eluted with CH_3OH−H_2O (60:40). Fr.C4 (213 mg) was fractionated by a Sephadex LH-20 column ($CHCl_3$−CH_3OH, 1:1), a silica gel column (CH_3OH−H_2O, 94:6) followed by a RP-18 column using CH_3OH−H_2O (60:40), furnishing **5** (22 mg). Fractions D and E combined (295 mg) were chromatographed over a Sephadex LH-20 column

https://dx.doi.org/10.1021/acs.jafc.0c00592
J. Agric. Food Chem. 2020, 68, 4624−4631

Table 1. ^{1}H NMR Spectroscopic Data for Compounds 2−7

no.	δ_H (J in Hz)	δ_H (J in Hz)	δ_H (J in Hz)	δ_H (J in Hz)	δ_H (J in Hz)	δ_H (J in Hz)
	2[a]	**3**[b]	**4**[c]	**5**[b]	**6**[b]	**7**[c]
1α	1.70−1.76[d]m	1.73−1.79[d]m	1.77−1.81 m	1.69−1.73[d]m	1.72−1.77[d]m	1.70 d (9.5)
1β	0.92 dd (13.4, 4.1)	1.31−1.35 m	0.86 s	0.84−0.89 m	0.90−0.97 m	0.92 dd (13.4, 3.8)
2	1.32−1.38[d](m)	1.38−1.42 m	1.29−1.32[d]m	1.36−1.43[d]m	1.35−1.38 m	1.31−1.38[d]m
	1.81−1.90[d](m)	1.85−1.90 m	1.84−1.91[d]m	1.83−1.88[d]m	1.88−1.90 m	1.78−1.90[d]m
3	0.99−1.03[d](m)	0.99 td (13.3, 4.1)	0.93−0.99 m	0.98−1.04[d]m	0.99−1.09[d]m	0.99−1.04[d]m
	2.11, d (13.2)	1.73−1.79[d]m	2.11 d (13.2)	2.12 d (13.3)	2.11 d (13.2)	2.18 d (13.1)
5β	1.06 dd (11.9, 2.1)	1.71−1.76[d]m	1.01−1.04 m	0.98−1.04[d]m	0.99−1.09[d]m	1.11 dd (11.5, 3.04)
6	1.72−1.87[d](m)	1.71−1.79[d]m	1.66−1.73[d]m	1.67−1.73[d]m	1.61−1.69[d]m	1.74−1.84[d]m
				1.97−2.0 m		
7α	1.48−1.52[d]m	1.46 td (12.8, 5.8)	1.45−1.52[d]m		1.43−1.49 m	1.49−1.53[d]m
7β	1.31−1.36[d]m	1.14−1.18[d]m	1.34−1.38 m	3.22 dd (8.1, 2.8)	1.23−1.31 m	1.31−1.35[d]m
9β	0.97−1.03[d]m		1.09 dd (11.9, 1.9)	1.13−1.15[d]m	0.99−1.09[d]m	0.98−1.03[d]m
11	1.51−1.56[d]m	1.31−1.35 m	1.29−1.32[d]m	1.55−1.59 m	1.61−1.69[d]m	1.51−1.59[d]m
	1.62−1.70[d]m	2.01−2.06[d]m	1.84−1.91[d]m	1.73−1.80[d]m	1.83−1.85[d]m	1.64−1.71[d]m
12	1.13−1.19 m	1.43−1.49 m		1.15−1.19[d]m	1.13−1.15 m	1.13−1.18 m
	1.75−1.79[d]m	1.57−1.60 m	3.74 br t (1.2)	1.75−1.80[d]m	1.83−1.85[d]m	1.78 m
14	1.28 dd (11.5, 2.7)	0.82 dd (11.6, 2.5)	0.90−1.93 m	0.81 dd (7.6, 1.7)	2.99 s	1.27 dd (11.0, 2.5)
		1.94 dd (11.6, 3.2)	1.60−1.64 m	1.84−1.88[d]m		
15	1.66−1.70[d]m	1.76−1.79[d]m	1.66−1.73[d]m	2.25 br t (11.1)	1.72−1.77[d]m	1.64−1.71[d]m
	1.83−1.87[d]m	2.01−2.06[d]m	1.84−1.91[d]m	1.38−1.42[d]m	1.83−1.85[d]m	1.82−1.89[d]m
16β	3.79 dd (10.8, 4.6)	3.77 dd (10.8, 4.2)	3.88 dd (10.9, 4.4)	3.74 dd (7.3, 3.4)	4.11 t (7.4)	3.78 dd (11.4, 4.6)
17-CH_3	0.89 s	0.90 s	0.99 s	0.89 s	0.95 s	0.88 s
18-CH_3	1.17 s	1.17 s	1.17 s	1.19 s	1.17 s	1.20 s
20-CH_3	0.85 s	1.06 s	0.84 s	0.84 s	0.87 s	0.84 s
1′						5.4 d (8.0)
2′						3.30−3.37 m
3′						3.39 d (1.7)
4′						3.34−3.38[d]m
5′						3.32−3.38[d]m
6′						3.80 td (3.7, 1.7)
						3.67 td (4.4, 4.3)

[a]Measured at 500 MHz in methanol-d_4. [b]Measured at 600 MHz in methanol-d_4. [c]Measured at 400 MHz in methanol-d_4. [d]Overlapping.

($CHCl_3$−CH_3OH, 1:1) and silica gel CC elutingwith $CHCl_3$−CH_3OH (90:10) to yield **7** (4 mg).

The procedures were similar to those described above. From 100 mg of **1**, a crude extract was obtained, which was separated by silica gel CC eluting with a gradient of petroleum ether−acetone. Eluting with petroleum ether−acetone (9:1) led to the recovery of substrate **1** (50 mg). Further elution with petroleum ether−acetone (8:2) gave metabolites **8** (16 mg), **9** (3 mg), and **10** (3 mg).

ent-9α,16β-Dihydroxybeyeran-19-oic acid (**3**): white needle crystal (MeOH−EtOAc); $[\alpha]_D^{23}$ −45 (c 0.3, MeOH); IR (KBr): ν_{max} 3476, 3384 (OH), 2932, 2874, 1695 (COOH), 1455 cm^{-1}; ^{13}C and ^{1}H NMR data: see Tables 1 and 2; ESIMS m/z: 359.2 $[M + Na]^+$, 335.0 $[M - H]^-$; HRESIMS m/z: 335.2232 $[M - H]^-$ (calcd for $C_{20}H_{31}O_4$, 335.2228).

ent-12α,16β-Dihydroxybeyeran-19-oic acid (**4**): white needle crystal (MeOH); $[\alpha]_D^{23}$ −71 (c 0.3, MeOH); IR (KBr): ν_{max} 3491 (OH), 2946, 2845, 1702 (COOH), 1245 cm^{-1}; ^{13}C and ^{1}H NMR data: see Tables 1 and 2; ESIMS m/z: 359.1 $[M + Na]^+$, 335.1 $[M - H]^-$; HRESIMS m/z: 335.2238 $[M - H]^-$ (calcd for $C_{20}H_{31}O_4$, 335.2228).

ent-7β,16β-Dihydroxybeyeran-19-oic acid (**5**): white needle crystal (MeOH); $[\alpha]_D^{23}$ −60 (c 0.3, MeOH); IR (KBr): ν_{max} 3413 (OH), 2937, 2869, 1701 (COOH), 1455, 1193, 1069 cm^{-1}; ^{13}C and ^{1}H NMR (150, 600 MHz, CD_3OD) data: see Tables 1 and 2; ESIMS m/z: 359.2 $[M + Na]^+$, m/z: 335.1 $[M - H]^-$; HRESIMS m/z: 335.2231 $[M - H]^-$ (calcd for $C_{20}H_{31}O_4$, 335.2228).

ent-14β,16β-Dihydroxybeyeran-19-oic acid (**6**): white needle crystal (MeOH); $[\alpha]_D^{23}$ −54 (c 0.3, MeOH); IR (KBr): ν_{max} 3452 (OH), 2951, 2926, 2844, 1697 (COOH), 1460 cm^{-1}; ^{13}C and ^{1}H NMR data: see Tables 1 and 2; ESIMS m/z: 359.1 $[M + Na]^+$, 335.1 $[M-H]^-$; HRESIMS m/z: 335.2232 $[M - H]^-$ (calcd for $C_{20}H_{31}O_4$, 335.2228). All NMR data were in agreement with the literature data.[10]

ent-16β-Hydroxybeyeran-19-α-D-glucopyranosyl ester (**7**): white solid powder (MeOH); $[\alpha]_D^{23}$ −40 (c 0.3, MeOH); IR (KBr): ν_{max} 3420 (OH), 1725 (ester), 1073 cm^{-1}; ^{13}C and ^{1}H NMR data: see Tables 1 and 2; ESIMS m/z: 505.2 $[M + Na]^+$, 184.9 $[Glu + Na]^+$, 481.0 $[M - H]^-$, 319.0 $[M - Glu]^-$; HRESIMS m/z: 481.2809 $[M - H]^-$ (calcd for $C_{26}H_{41}O_8$, 481.2805). All NMR data were in accordance with the literature data.[12]

ent-9α-Hydroxy-16-ketobeyeran-19-oic acid (**8**): white needle crystal (MeOH); IR (KBr) ν_{max}: 3504, 3448 (OH), 2995, 2922, 2867, 1719 (CO), 1689 (COOH), 1451, 1254, 1142 cm^{-1}; ^{13}C NMR (125, acetone-d_6) data: see Table 2; ESIMS m/z: 357.1 $[M + Na]^+$, 335.1 $[M + H]^-$, 317.1 $[M - OH]^+$. All NMR data were concordant with the literature data.[11]

X-ray Crystallographic Data for Compounds 3 and 4. The crystals of **4** were obtained from MeOH−H_2O (3:1) and those of **3** from MeOH. The method used for structure analysis and the detailed crystallographic data are described in the Supporting Information.

Crystal data for **3**: $C_{21}H_{36}O_5$, M = 368.50, colorless crystals, orthorhombic, a = 8.0964(9) Å, b = 14.0282(13) Å, c = 17.5127(17) Å, α = 90.00°, β = 90.00°, γ = 90.00°, V = 1989.1(3) Å^3, space group $P2_12_12_1$, λ(Mo Kα) = 0.71073 Å, T = 298(2) K, Z = 4, μ = 0.086 mm^{-1}, 10062 reflections collected, 2024 independent reflections (R_{int} = 0.0338). Final R indices ($I > 2\sigma(I)$): R_1 = 0.0366, wR_2 = 0.0806. Final R indices (all data): R_1 = 0.0561, wR_2 = 0.0949. Goodness of fit on F^2: 1.078. Flack parameter: −3.1(18). Crystallographic data for **3**

https://dx.doi.org/10.1021/acs.jafc.0c00592
J. Agric. Food Chem. 2020, 68, 4624−4631

Table 2. ^{13}C NMR Spectroscopic Data for Compounds 2−8

no.	δ_C type	δ_C type	δ_C type	δ_C type	δ_C type	δ_C type	δ_C type
	2[a]	**3**[b]	**4**[c]	**5**[b]	**6**[b]	**7**[c]	**8**[d]
1	41.3 t	38.9 t	41.0 t	40.9 t	41.4 t	41.1 t	32.4 t
2	20.1 t	20.1 t	20.0 t	20.0 t	20.1 t	20.0 t	20.2 t
3	39.2 t	37.9 t	39.2 t	39.0 t	39.1 t	39.0 t	38.6 t
4	44.6 s	44.8 s	44.7 s	44.4 s	44.6 s	45.1 s	41.1 s
5	58.4 d	49.6 d	58.4 d	56.6 d	58.0 d	58.9 d	48.8 d
6	23.0 t	22.9 t	23.0 t	32.0	22.3 t	22.8 t	22.6 t
7	43.0 t	33.0 t	42.6 t	76.6 d	37.4 t	43.0 t	37.1 t
8	43.1 s	47.8 s	43.6 s	49.1 s	47.6 s	43.1 s	48.6 s
9	57.4 d	78.9 s	52.3 d	55.4 d	56.9 d	57.4 d	76.7 s
10	39.4 s	44.5 s	38.9 s	39.4 s	39.4 s	39.4 s	44.1 s
11	21.4 t	26.8 t	29.7 t	21.1 t	21.0 t	21.4 t	26.8 t
12	34.9 t	31.3 t	72.3 d	34.7 t	34.3 t	35.0 t	33.8 t
13	43.2 s	42.8 s	47.6 s	42.5 s	47.7 s	43.2 s	45.1 s
14	56.6 t	49.3 t	49.7 t	51.1 t	79.6 d	56.6 t	48.3 t
15	43.6 t	45.8 t	42.8 t	33.7 t	41.4 t	43.4 t	50.6 t
16	81.0 d	80.2 d	81.4 d	80.9 d	92.9 d	81.1 d	220.7 s
17	25.4 q	25.2 q	22.2 q	25.4 q	20.2 q	25.4 q	19.7 q
18	29.6 q	29.8 q	29.6 q	29.5 q	29.6 q	29.3 q	29.5 q
19	181.7 s	182.0 s	181.8 s	181.5 s	181.7 s	178.2 s	179.3 s
20	13.9 q	17.4 q	13.9 q	14.0 q	14.2 q	14.3 q	17.0 q
1′						95.6 d	
2′						74.0 d	
3′						78.7 d	
4′						71.1 d	
5′						78.6 d	
6′						62.4 t	

[a]Measured at 125 MHz in methanol-d_4. [b]Measured at 150 MHz in methanol-d_4. [c]Measured at 100 MHz in methanol-d_4. [d]Measured at 125 MHz in acetone-d_6.

have been deposited with the Cambridge Crystallographic Data Center as supplementary publication number CCDC-773007.

Crystal data for **4**: $C_{21}H_{36}O_5$, M = 368.50, colorless needles, orthorhombic, a = 6.7541(8) Å, b = 13.6991(17) Å, c = 21.781(3) Å; α = 90.00°, β = 90.00°, γ = 90.00°, V = 2015.3(4) Å^3, space group $P2_12_12_1$, λ(Mo Kα) = 0.71073 Å, T = 296.15(2) K, Z = 4, μ = 0.085 mm^{-1}, 10,615 reflections collected, 3824 independent reflections (R_{int} = 0.0194). Final R indices ($I > 2\sigma(I)$): R_1 = 0.0418, wR_2 = 0.1184. Final R indices (all data): R_1 = 0.0471, wR_2 = 0.1238. Goodness of fit on F^2: 1.065. Flack parameter: −0.4(4). Crystallographic data for **4** have been deposited with the Cambridge Crystallographic Data Center as supplementary publication number CCDC-804761.

α-Glucosidase Inhibitory Assay. The α-glucosidase inhibition test of the compounds was carried out as reported previously.[17,18] Briefly, *Saccharomyces cerevisiae* α-glucosidase was supplied by Sigma (EC 3.2.1.20). A solution of the enzyme in 200 μL of 10 mM phosphate buffer (pH 6.80) was incubated with 12 μL of the compound tested in dimethylsulfoxide at 37 °C for 5 min. After the addition of 36 μL of 4-nitrophenyl α-D-glucopyranoside, the reaction was maintained at 37 °C for 40 min. The released 4-nitrophenol amount was examined at 400 nm. The test was carried out with five different concentrations around the IC_{50} values. In each set of experiments, the bioassay was conducted in triplicate. The IC_{50} values were calculated as described previously.[17]

Neurite-Outgrowth Assay. The cell viability assay was performed to examine the cytotoxicity of the tested compounds in PC-12 cells (Shanghai Institutes for Biological Sciences, Shanghai) according to the MTT assay.[19,20] Morphological analysis and quantification of neurite-bearing cells were carried out by using a phase-contrast microscope according to previous reported procedures.[21] Briefly, PC-12 cells were seeded on poly-L-lysine-coated 24-well plates (2×10^4 cells/mL) in DMEM containing 10% HS, 5% FBS, 100 μg/mL streptomycin, and 100 IU/mL penicillin at 37 °C under 5% CO_2 and a humidified atmosphere of 95% air for 24 h. Cells without treatment were used as a negative control. Cells treated with nerve growth factor (NGF; 20 ng/mL) were employed as a positive control. One concentration experiment was repeated in three wells. After further 72 h incubation, neurite outgrowth in PC-12 cells was observed under an inverted microscope, and five images were chosen randomly under a microscope for each well. At least 100 cells in each of five randomly separated fields were scored, and the cells with neurites equal to or greater than the length of one cell body were positive for neurite outgrowth and expressed as a percentage of the total cell number in five fields.

NO Inhibition Assay. The cell viability and inhibition of NO production in BV-2 cells were assayed as reported previously.[22]

Phytotoxicity Assay. Phytotoxic activity was tested by the previously described method.[23,24]

RESULTS AND DISCUSSION

Initial screening biotransformation of 11 organisms indicated that the fungal strain *C. echinulata* ATCC 8688a was able to transform substrate **1** or **2** into several metabolites. As a result, they were selected for detailed studies of the scale-up conversion of **2**. Preparative incubation of the substrates, **1** and **2**, with *C. echinulata* resulted in the isolation of three new metabolites, **3**−**5**, as well as five known ones, **6**−**10** (Scheme 1). Assignments of all of the ^1H and ^{13}C NMR data for the new metabolites (Tables 1 and 2) described here were done from DEPT, $^1H-^1H$ COSY, HSQC, HMBC, and NOESY correlations. The known compounds were determined to be *ent*-14β,16β-dihydroxybeyeran-19-oic acid (**6**), *ent*-16β-hydroxybeyeran-19-β-D-glucopyranosyl ester (**7**), *ent*-9α-hydroxy-16-ketobeyeran-19-oic acid (**8**), *ent*-7α-hydroxy-16-ketobeyeran-19-oic acid (**9**), and *ent*-7β-hydroxy-16-ketobeyer-

https://dx.doi.org/10.1021/acs.jafc.0c00592
J. Agric. Food Chem. 2020, 68, 4624−4631

an-19-oic acid (**10**) by comparison of the NMR and ESIMS data with the literature.[10−12,16]

Metabolite **3** showed the molecular formula of $C_{20}H_{32}O_4$, as deduced from its HRESIMS *m*/*z*: 335.2232 $[M - H]^-$ and ^{13}C NMR data, suggesting that **3** contained one more oxygen atom than **2**. The IR spectrum showed absorptions typical of carbonyl (1695 cm^{-1}) and hydroxyl groups (3476, 3384 cm^{-1}), revealing that a hydroxylation had taken place and that the carboxylic groups were not affected. The ^1H NMR spectrum of **3** (Table 1) displayed three methyl signals characteristic of H_3-17 (δ_H 0.90), H_3-20 (δ_H 1.06), and H_3-18 (δ_H 1.17). The ^{13}C NMR (DEPT) spectra of **3** (Table 2) displayed the presence of 20 carbon signals including three tertiary methyls, nine methylenes, two methines, and six quaternary carbons. In comparison with the ^1H and ^{13}C NMR spectra of **2** and **3**, one CH signal at δ_C 57.4 and δ_H 0.97−1.03 in **2** was replaced by one hydroxyl-bearing carbon signal at δ_C 78.9 in **3**, suggesting the new OH group to be located at C-9. Furthermore, in the ^{13}C NMR spectrum, the resonances of C-8, C-9, C-10, and C-11 shifted significantly downfield from δ_C 43.1 to 47.8, from δ_C 57.4 to 78.9, from δ_C 39.3 to 44.5, and from δ_C 21.4 to 26.9, respectively, and the resonances of C-1, C-7, and C-14 shifted upfield from δ_C 41.3 to 38.9, from δ_C 43.0 to 33.0, and from δ_C 56.5 to 49.3, respectively. Consequently, the tertiary hydroxyl group was located at C-9. This deduction was confirmed by the HMBC correlations of H_2-1, H_2-11, H_2-12, H_2-14, and H_3-20 with C-9 (Figure 1). Furthermore, the structure of **3** was confirmed by X-ray crystallographic data (Figure 2). Therefore, **3** was assigned as *ent*-9*α*,16*β*-dihydroxybeyeran-19-oic acid.

Metabolite **4** showed the molecular formula of $C_{20}H_{32}O_4$, as deduced from its HRESIMS *m*/*z*: 335.2238 $[M - H]^-$ and ^{13}C NMR spectra, indicating one more oxygen atom than **2**. The IR spectrum showed absorptions typical of carbonyl (1702 cm^{-1}) and hydroxyl groups (3491 cm^{-1}), indicating that a hydroxylation had taken place and that the carboxyl group was not affected. The ^1H NMR spectrum of **3** (Table 1) displayed characteristic signals of three methyls H_3-20 (δ_H 0.84), H_3-17 (δ_H 0.99), and H_3-18 (δ_H 1.17). The ^{13}C NMR (DEPT) spectra of **4** (Table 2) displayed the presence of 20 carbon signals including three tertiary methyls, eight methylenes, four methines, and five quaternary carbons. Compared to the ^1H NMR and DEPT spectra of **2** (Tables 1 and 2), the disappearance of one CH_2 signal at δ_C 34.9 and δ_H 1.13−1.19 (m) and 1.75−1.79 (m) in **2**, which was replaced by one hydroxyl-bearing methine signal at δ_C 72.3 and δ_H 3.74 (br. t, *J* = 1.2 Hz) in **4**, suggesting the additional OH group to be attached at C-12. Furthermore, the resonances of C-11 and C-13 shifted downfield from δ_C 21.4 to 29.7 and from δ_C 43.2 to 47.5, respectively, and the resonances of C-9, C-14, and C-17 shifted upfield from δ_C 57.4 to 52.3, from δ_C 56.6 to 49.7, and from δ_C 25.4 to 22.2, respectively. As a result, the hydroxyl group was located at C-12. This deduction was also confirmed by the COSY correlations of H-12 (δ_H 3.74) with the H_2-11 (δ_H 1.64−1.71 and 1.84−1.91) (Figure 1). Irradiation of the signal of *α*-orientated H-16 (δ_H 3.88) led to a NOE enhancement of a small broad triplet signal at H-12 (δ_H 3.74, 100%), thereby indicating the 12-OH group to be in the axial (*β*) position. Finally, the structure of **4** was confirmed by X-ray crystallographic analysis (Figure 3). Thus, **4** was established as *ent*-12*α*,16*β*-dihydroxybeyeran-19-oic acid.

Metabolite **5** showed the molecular formula of $C_{20}H_{32}O_4$, as deduced from its HRESIMS *m*/*z*: 335.2231 $[M - H]^-$.

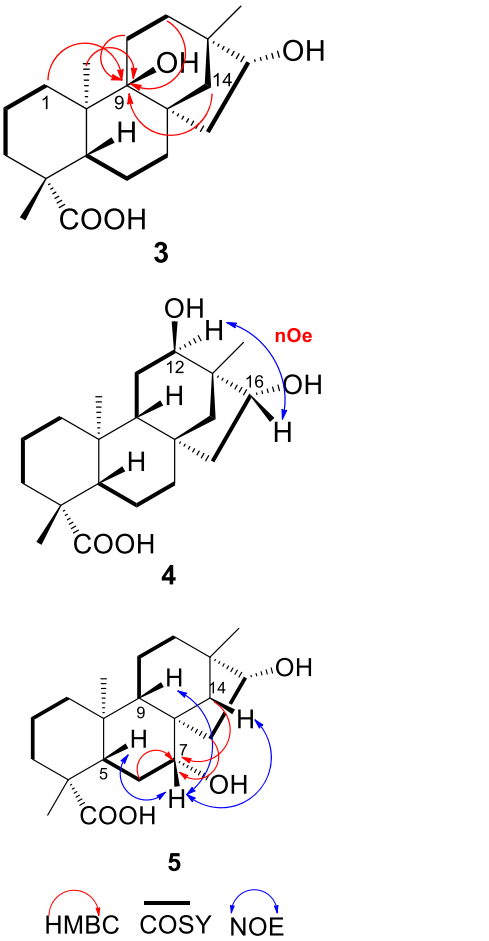

Figure 1. Selected HMBC, NOESY, and COSY correlations for **3**−**5**.

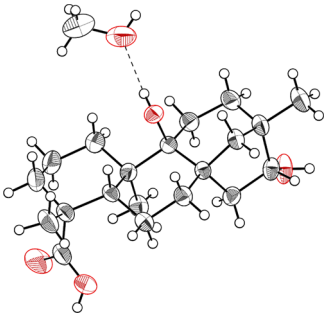

Figure 2. ORTEP drawing of the X-ray structures of **3**.

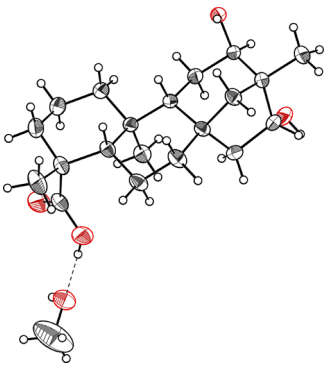

Figure 3. ORTEP drawing of the X-ray structures of **4**.

https://dx.doi.org/10.1021/acs.jafc.0c00592
J. Agric. Food Chem. 2020, 68, 4624−4631

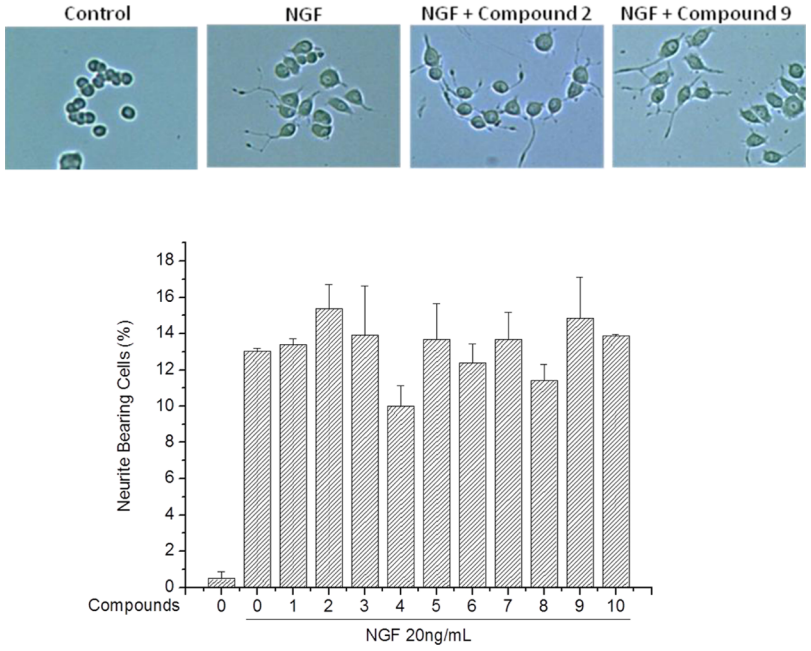

Figure 4. Effect of compounds **1**−**10** on the NGF-induced neurite outgrowth in PC12 cells. (Top) Morphological change of PC12 cells treated with **2** and **9** at 20 μM. The cell morphological characteristics were observed under a light microscope. (Bottom) Percentage of neurite outgrowth of PC12 cells after treatment with compounds **1**−**10** at 20 μM in the presence of NGF for 72 h.

Examination of DEPT and HSQC spectra of **5** indicated that a monohydroxylation had occurred. Comparison of ^{1}H and ^{13}C NMR spectra of **2** and **5** revealed that the substitution of an additional hydroxyl group in **5** might be at C-7. This coincided with the ^{13}C NMR signals observed for downfield shifts of C-6 ($\Delta\delta$ +9.0) and C-8 ($\Delta\delta$ +6.0) and upfield shifts of C-5 ($\Delta\delta$ −1.8), C-9 ($\Delta\delta$ −2.0), C-14 ($\Delta\delta$ −5.5), and C-15 ($\Delta\delta$ −9.9), respectively, in comparison with those of **2** (Table 2). In the HMBC spectrum, H-7 at δ_H 3.22 exhibited cross-peaks with C-6 (δ_C 32.0), C-9 (δ_C 55.4), C-14 (δ_C 51.1), and C-15 (δ_C 33.7) (Figure 1). Therefore, the hydroxylation occurred at C-7 (δ_C 76.6). In the ^{1}H NMR spectrum, the α-configuration of the OH group at C-7 was deduced from the double-doublet multiplicity of the C-7 signal (1H, dd, J = 8.1, 2.8 Hz) in **5**.[6] Furthermore, the relative stereochemistry of OH-7 was also confirmed by a NOESY experiment (Figure 1), in which H-7 (δ_H 3.22) showed obvious correlations with H-5 (δ_H 1.01), H-9 (δ_H 1.14), and H-14 (δ_H 0.81). Thus, the structure of **5** was established to be *ent*-7β,16β-dihydroxybeyeran-19-oic acid.

Metabolite **7** has a molecular formula of $C_{26}H_{42}O_8$, as determined by HRESIMS at m/z: 481.2809 $[M - H]^-$. Six additional resonances in the ^{13}C NMR spectra of **7** (Table 2) revealed a hexose moiety in the structure. The hexose moiety was verified to be characteristic of ß-D-glucose by the NMR spectra. The coupling constant of the anomeric proton at δ_H 5.4 ppm (d, J = 8.0 Hz, H-1′) of the glucose residue in **7** disclosed the ß-configuration of the glucosidic linkage. Comparison of the ^{13}C NMR spectra of compounds **2** and **7** suggested that **7** was a glucopyranosyl ester of **2** at C-19 due to the upfield shift of C-19 from 181.7 to 178.2 ppm (Table 2). Based on the above evidence and literature data,[12] the structure of **7** was characterized as shown. This is the first report to obtain the glucosidation of **2** by *C. echinulata*.

An array of microbial transformations of the two beyerane-type diterpenoids, especially isosteviol (**1**), involved oxidation reactions by different species of microorganisms, such as *Mortierella isabellina*,[10] *Actinoplanes* sp., *Mucor recurvatus*, *Cunninghamella bainieri*,[11] *Bacillus megaterium*, *A. niger*,[12] *Gibberella fujikuroi*,[15] and *Glomerella cingulata* and *Mortierella elongate*.[25,26] These species have the capacity of functionalizing **1** or **2** at the C-7 or C-9 position. This is a common occurrence for other microorganisms with beyerane-type scaffolds.[4,6,16]

In this study, *C. echinulata* was accountable for the most common biohydroxylation reactions that took place in the microbial conversions, and several hydroxylated *ent*-beyerane congeners (**3**−**8**) were prepared regio- and stereoselectively by hydroxylation at 9β-, 12β-, 14α-, 7α- and 7α-, 7β-, 9β-positions on the *ent*-beyerane skeleton by using this strain. Interestingly, it has been reported that some xenobiotics are known to generate conjugates with glucose in mammalian systems.[12,27] Selected microbes, especially fungi, have been employed successfully as *in vitro* models to predict and imitate the metabolic fate of drugs and other xenobiotics in mammalian systems.[28−30] Compound **7**, a conjugated fungal metabolite of **2**, had been obtained previously through glucosidation by the bacterium *B. megaterium*.[12] However, the glycoside formation by *C. echinulata* has been first reported for the tetracyclic beyerane diterpene motifs.

We next tested the neurite-outgrowth promoting, α-glucosidase and NO production inhibiting, and phytotoxic effects of the transformation products. Results showed that only compounds **2** and **9** were found to promote neurite-outgrowth effects in the presence of NGF in PC-12 cells, the others did not display any activity (Figure 4). The prevalence of neurodegenerative diseases (ND), such as Alzheimer's disease, will continue to increase steadily. Despite the advancement of treatment, the management of these disorders remains highly ineffective. Therefore, it is essential to discover new biologically active natural products and analogues thereof to mitigate ND. Over the past decades, neurotrophic factors, for example, NGF, have attracted great interest because of their

https://dx.doi.org/10.1021/acs.jafc.0c00592
J. Agric. Food Chem. 2020, 68, 4624−4631

therapeutic potentials in regulating the growth, differentiation, and survival of cells in the central nervous system.[26] However, these high-molecular polypeptides cannot cross the brain blood barrier in addition to their degradation under physiological conditions.[27] To address this issue, considerable endeavors have been made to discover low-molecular molecules that display neurotrophic effects and/or that are capable of improving the effects of endogenous neurotrophic factors.

In summary, we demonstrated for the first time that eight oxygenated metabolites were obtained and characterized from the scale-up bioconversion of isosteviol (**1**) and *ent*-16β-hydroxybeyeran-19-oic acid (**2**) with *C. echinulata*. The bioreactions were associated not only with stereoselective introduction of hydroxyl groups at positions C-7, -9, -12, and -14 but also with glucosidation at C-19 of **2**.

■ ASSOCIATED CONTENT

Supporting Information

The Supporting Information is available free of charge at https://pubs.acs.org/doi/10.1021/acs.jafc.0c00592.

Experimental details of assays and 1D NMR, 2D NMR, and HRESIMS spectra for **3**−**5** (PDF)

X-ray crystallographic data for **3** (CIF)

X-ray crystallographic data for **4** (CIF)

■ AUTHOR INFORMATION

Corresponding Author

Jin-Ming Gao − *Shaanxi Key Laboratory of Natural Products & Chemical Biology, College of Chemistry & Pharmacy, Northwest A&F University, Yangling 712100, Shaanxi, People's Republic of China*; orcid.org/0000-0003-4801-6514; Phone: 86-29-87092335; Email: jinminggao@nwsuaf.edu.cn

Authors

Yu-Qi Gao − *Shaanxi Key Laboratory of Natural Products & Chemical Biology, College of Chemistry & Pharmacy, Northwest A&F University, Yangling 712100, Shaanxi, People's Republic of China*

Ruoxin Li − *Shaanxi Key Laboratory of Natural Products & Chemical Biology, College of Chemistry & Pharmacy, Northwest A&F University, Yangling 712100, Shaanxi, People's Republic of China*

Wei-Wei Wang − *Shaanxi Key Laboratory of Natural Products & Chemical Biology, College of Chemistry & Pharmacy, Northwest A&F University, Yangling 712100, Shaanxi, People's Republic of China*

Shoei-Sheng Lee − *School of Pharmacy, College of Medicine, National Taiwan University, Taipei 10051, Taiwan, ROC*

Complete contact information is available at: https://pubs.acs.org/10.1021/acs.jafc.0c00592

Funding

This research was financially supported by the Fundamental Research Funds for the Central Universities (2452019185).

Notes

The authors declare no competing financial interest.

■ REFERENCES

(1) Well, C.; Frank, O.; Hofmann, T. Quantitation of sweet steviol glycosides by means of a HILIC-MS/MS-SIDA approach. *J. Agri. Food Chem.* **2013**, *61*, 11312−11320.

(2) Wölwer-Rieck, U. The leaves of *Stevia rebaudiana* (Bertoni), their constituents and the analyses thereof: a review. *J. Agric. Food Chem.* **2012**, *60*, 886−895.

(3) Zhang, H.; Zhong, K.; Lu, M.; Mei, Y.; Tan, E.; Sun, X.; Tan, W. Neuroprotective effects of isosteviol sodium through increasing CYLD by the downregulation of miRNA-181b. *Brain Res. Bull.* **2018**, *140*, 392−401.

(4) Hanson, J. R. The microbiological transformation of diterpenoids. *Nat. Prod. Rep.* **1992**, *9*, 139−152.

(5) Rico-Martínez, M.; Medina, F. G.; Marrero, J. G.; Osegueda-Robles, S. Biotransformation of diterpenes. *RSC Adv.* **2014**, *4*, 10627−10647.

(6) De Oliveira, B.; Santos, M. C.; Leal, P. C. Biotransformation of the diperpenoid, isosteviol, by Aspergillus niger, Penicillium chrysogenum and Rhizopus arrhizus. *Phytochemistry* **1999**, *51*, 737−741.

(7) Wu, G.-W.; Gao, J.-M.; Shi, X.-W.; Zhang, Q.; Wei, S.-P.; Ding, K. Microbial Transformations of Diosgenin by the White-Rot BasidiomyceteCoriolus versicolor. *J. Nat. Prod.* **2011**, *74*, 2095−2101.

(8) Yang, L.-M.; Chang, S.-F.; Lin, W.-K.; Chou, B.-H.; Wang, L.-H.; Liu, P.-C.; Lin, S.-J. Oxygenated compounds from the bioconversion of isostevic acid and their inhibition of TNF-α and COX-2 expressions in LPS-stimulated RAW 264.7 cells. *Phytochemistry* **2012**, *75*, 90−98.

(9) Li, X.-J.; Shi, X. W.; Shuai, Q.; Gao, J. M.; Zhang, A. L. Bioactive metabolites from biotransformation of paeonol by the white-rot basidiomycete *Coriolus versicolor*. *Nat. Prod. Commun.* **2011**, *6*, 1129−1130.

(10) Lin, C.-L.; Lin, S.-J.; Huang, W.-J.; Ku, Y.-L.; Tsai, T.-H.; Hsu, F.-L. Novel ent-beyeran-19-oic acids from biotransformations of isosteviol metabolites by Mortierella isabellina. *Planta Med.* **2007**, *73*, 1581−1587.

(11) Hsu, F.-L.; Hou, C.-C.; Yang, L.-M.; Cheng, J.-T.; Chi, T.-C.; Liu, P.-C.; Lin, S.-J. Microbial transformations of isosteviol. *J. Nat. Prod.* **2002**, *65*, 273−277.

(12) Yang, L. M.; Hsu, F. L.; Cheng, J. T.; Chang, C. H.; Liu, P. C.; Lin, S. J. Hydroxylation and glucosidation of *ent*-16β-hydroxybeyeran-19-oic acid by *Bacillus megaterium* and *Aspergillus niger*. *Planta Med.* **2004**, *70*, 359−363.

(13) Chou, B.-H.; Yang, L.-M.; Chang, S.-F.; Hsu, F.-L.; Lo, C.-H.; Liaw, J.-H.; Liu, P.-C.; Lin, S.-J. Microbial transformation of isosteviol lactone and evaluation of the transformation products on androgen response element. *J. Nat. Prod.* **2008**, *71*, 602−607.

(14) Wonganan, O.; Tocharus, C.; Puedsing, C.; Homvisasevongsa, S.; Sukcharoen, O.; Suksamrarn, A. Potent vasorelaxant analogs from chemical modification and biotransformation of isosteviol. *Eur. J. Med. Chem.* **2013**, *62*, 771−776.

(15) Ali, M. S.; Hanson, J. R.; de Oliveira, B. H. The biotransformation of some *ent*-beyeran-19-oic acids by *Gibberella fujikuroi*. *Phytochemistry* **1992**, *31*, 507−510.

(16) de Oliveira, B. H.; Strapasson, R. A. Biotransformation of isosteviol by *Fusarium verticilloides*. *Phytochemistry* **1996**, *43*, 393−395.

(17) Wei, J.; Zhang, X.-Y.; Deng, S.; Cao, L.; Xue, Q.-H.; Gao, J.-M. α-Glucosidase inhibitors and phytotoxins from Streptomyces xanthophaeus. *Nat. Prod. Res.* **2017**, *31*, 2062−2066.

(18) Yin, H.; Dan, W.-J.; Fan, B.-Y.; Guo, C.; Wu, K.; Li, D.; Xian, K.-F.; Pescitelli, G.; Gao, J.-M. Anti-inflammatory and α-Glucosidase Inhibitory Activities of Labdane and Norlabdane Diterpenoids from the Rhizomes of Amomum villosum. *J. Nat. Prod.* **2019**, *82*, 2963−2971.

(19) Tang, J.-J.; Dong, S.; Han, Y.-Y.; Lei, M.; Gao, J.-M. Synthesis of 1-O-acetylbritannilactone analogues from *Inula britannica* and in vitro evaluation of their anticancer potential. *Med. Chem. Commun.* **2014**, *5*, 1584−1589.

(20) Han, Y.-Y.; Tang, J.-J.; Gao, R.-F.; Guo, X.; Lei, M.; Gao, J.-M. A new semisynthetic 1- O -acetyl-6- O -lauroylbritannilactone induces apoptosis of human laryngocarcinoma cells through p53-dependent pathway. *Toxicol. In Vitro.* **2016**, *35*, 112−120.

(21) Bai, R.; Zhang, C.-C.; Yin, X.; Wei, J.; Gao, J.-M. Striatoids A-F, Cyathane Diterpenoids with Neurotrophic Activity from Cultures of the Fungus Cyathus striatus. *J. Nat. Prod.* **2015**, *78*, 783−788.
(22) Tang, D.; Liu, L.-L.; He, Q.-R.; Yan, W.; Li, D.; Gao, J.-M. Ansamycins with antiproliferative and antineuroinflammatory activity from Moss-Soil-Derived Streptomyces cacaoi subsp. asoensis H2S5. *J. Nat. Prod.* **2018**, *81*, 1984−1991.
(23) Li, H.; Wei, J.; Pan, S.-Y.; Gao, J.-M.; Tian, J.-M. Antifungal, phytotoxic and toxic metabolites produced byPenicillium purpurogenum. *Nat. Prod. Res.* **2014**, *28*, 2358−2361.
(24) Han, W.-B.; Zhai, Y.-J.; Gao, Y.; Zhou, H.-Y.; Xiao, J.; Pescitelli, G.; Gao, J.-M. Cytochalasins and an abietane-type diterpenoid with allelopathic activities from the endophytic fungus *Xylaria* species. *J. Agric. Food Chem.* **2019**, *67*, 3643−3650.
(25) Akihisa, T.; Hamasaki, Y.; Tokuda, H.; Ukiya, M.; Kimura, Y.; Nishino, H. Microbial Transformation of Isosteviol and Inhibitory Effects on Epstein−Barr Virus Activation of the Transformation Products. *J. Nat. Prod.* **2004**, *67*, 407−410.
(26) Chang, S.-F.; Yang, L.-M.; Lo, C.-H.; Liaw, J.-H.; Wang, L.-H.; Lin, S.-J. Microbial transformation of isosteviol and bioactivities against the glucocorticoid/androgen response elements. *J. Nat. Prod.* **2008**, *71*, 87−92.
(27) Chatterjee, P.; Pezzuto, J. M.; Kouzi, S. A. Glucosidation of Betulinic Acid byCunninghamellaSpecies. *J. Nat. Prod.* **1999**, *62*, 761−763.
(28) Clark, A. M.; Hufford, C. D. Use of microorganisms for the study of drug metabolism: an update. *Med. Res. Rev.* **1991**, *11*, 473−501.
(29) Fumagalli, F.; Molteni, R.; Calabrese, F.; Maj, P. F.; Racagni, G.; Riva, M. A. Neurotrophic Factors in Neurodegenerative Disorders. *CNS Drugs* **2008**, *22*, 1005−1019.
(30) Calissano, P.; Matrone, C.; Amadoro, G. Nerve growth factor As a paradigm of neurotrophins related to Alzheimer's disease. *Develop. Neurobiol.* **2010**, *70*, 372−383.

https://dx.doi.org/10.1021/acs.jafc.0c00592
J. Agric. Food Chem. 2020, 68, 4624−4631